



Published in final edited form as:

*Bioorg Med Chem.* 2020 November 15; 28(22): 115710. doi:10.1016/j.bmc.2020.115710.

## Analogues of nitrofurantoin antibiotics are potent GroEL/ES inhibitor pro-drugs.

Mckayla Stevens<sup>a</sup>, Chris Howe<sup>a</sup>, Anne-Marie Ray<sup>a</sup>, Alex Washburn<sup>a</sup>, Siddhi Chitre<sup>a</sup>, Jared Sivinski<sup>b</sup>, Yangshin Park<sup>a,c,d</sup>, Quyen Q. Hoang<sup>a,c,d</sup>, Eli Chapman<sup>b</sup>, Steven M. Johnson<sup>a</sup>

<sup>a</sup>Indiana University School of Medicine, Department of Biochemistry and Molecular Biology, 635 Barnhill Dr., Indianapolis, IN 46202

<sup>b</sup>The University of Arizona, College of Pharmacy, Department of Pharmacology and Toxicology, 1703 E. Mabel St., PO Box 210207, Tucson, AZ 85721

<sup>c</sup>Stark Neurosciences Research Institute, Indiana University School of Medicine. 320 W. 15th Street, Suite 414, Indianapolis, IN 46202

<sup>d</sup>Department of Neurology, Indiana University School of Medicine. 635 Barnhill Drive, Indianapolis, IN 46202

### Abstract

In two previous studies, we identified compound **1** as a moderate GroEL/ES inhibitor with weak to moderate antibacterial activity against Gram-positive and Gram-negative bacteria including *Bacillus subtilis*, methicillin-resistant *Staphylococcus aureus*, *Klebsiella pneumoniae*, *Acinetobacter baumannii*, and SM101 *Escherichia coli* (which has a compromised lipopolysaccharide biosynthetic pathway making bacteria more permeable to drugs). Extending from those studies, we developed two series of analogues with key substructures resembling those of known antibacterials, nitrofurantoin (hydroxyquinoline moiety) and nifuroxazide/nitrofurantoin (*bis*-cyclic-*N*-acylhydrazone scaffolds). Through biochemical and cell-based assays, we identified potent GroEL/ES inhibitors that selectively blocked *E. faecium*, *S. aureus*, and *E. coli* proliferation with low cytotoxicity to human colon and intestine cells *in vitro*. Initially, only the hydroxyquinoline-bearing analogues were found to be potent inhibitors in our GroEL/ES-mediated

**Corresponding Author:** Steven M Johnson, johnstm@iu.edu, 317-274-2458.

**Publisher's Disclaimer:** This is a PDF file of an unedited manuscript that has been accepted for publication. As a service to our customers we are providing this early version of the manuscript. The manuscript will undergo copyediting, typesetting, and review of the resulting proof before it is published in its final form. Please note that during the production process errors may be discovered which could affect the content, and all legal disclaimers that apply to the journal pertain.

### 6. SUPPORTING INFORMATION

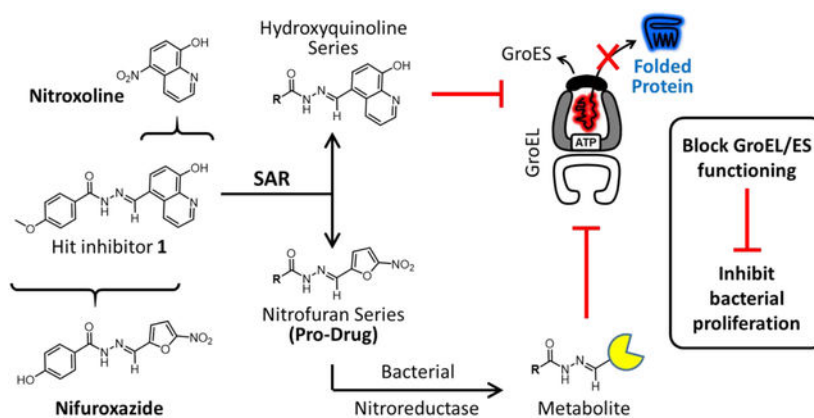
Supporting Information associated with this article can be found in the online version, which includes tabulation of all biochemical IC<sub>50</sub>, bacterial proliferation EC<sub>50</sub>, and human cell viability CC<sub>50</sub> values; log(IC<sub>50</sub>), log(EC<sub>50</sub>), and log(CC<sub>50</sub>) results with standard deviations; Correlation plots examining the selectivity of compounds inhibiting the proliferation of *E. faecium*, *S. aureus*, and *E. coli* over cytotoxicity to human FHC colon cells; *E. coli* resistance re-confirmation dose-response curves for nifuroxazide, nitrofurantoin, and compound **17**; results plotted for replicate 2 samples evaluating for cross-resistance between the respective resistant *E. coli* strains with nifuroxazide, nitrofurantoin, and compound **17**; characterization data for test compounds (MS, <sup>1</sup>H-NMR, and HPLC purity); detailed experimental protocols for protein synthesis and purification, and biochemical, bacterial proliferation, and human cell viability assays; and SMILES strings of compound structures.

### Declaration of interests

The authors declare that they have no known competing financial interests or personal relationships that could have appeared to influence the work reported in this paper.

substrate refolding assays; however, subsequent testing in the presence of an *E. coli* nitroreductase (NfsB) *in situ* indicated that metabolites of the nitrofuran-bearing analogs were potent GroEL/ES inhibitor pro-drugs. Consequently, this study has identified a new target of nitrofuran-containing drugs, and is the first reported instance of such a unique class of GroEL/ES chaperonin inhibitors. The intriguing results presented herein provide impetus for expanded studies to validate inhibitor mechanisms and optimize this antibacterial class using the respective GroEL/ES chaperonin systems and nitroreductases from *E. coli* and the *ESKAPE* bacteria.

## GRAPHICAL ABSTRACT



## Keywords

GroEL; GroES; molecular chaperone; chaperonin; proteostasis; small molecule inhibitors; *ESKAPE* pathogens; antibiotics; antibacterials; nitroreductase; pro-drugs

## 1. INTRODUCTION

The rise of antibiotic-resistant infections has become a significant threat to human health worldwide. This issue has been recently re-emphasized by the World Health Organization's 2019 report to Secretary-General of the United Nations "No time to wait: Securing the future from drug-resistant infections" and the Centers for Disease Control and Prevention (CDC) in their 2019 report titled "Antibiotic Resistance Threats in the United States".<sup>1, 2</sup> World-wide, over 700,000 deaths from drug-resistant infections occur annually.<sup>1</sup> In the US alone, more than 2.8 million infections by antibiotic resistant bacteria occur annually, with 35,000 deaths. Of particular prominence is a subset of bacteria referred to as the *ESKAPE* pathogens – an acronym that represents Gram-positive *Enterococcus faecium* and *Staphylococcus aureus* bacteria, and Gram-negative *Klebsiella pneumoniae*, *Acinetobacter baumannii*, *Pseudomonas aeruginosa*, and *Enterobacter* species.<sup>3–8</sup> While several classes of antibiotics that target diverse biological pathways have been successfully used to treat these bacteria for decades, we are in an era where derivatizing analogs to circumvent bacterial resistance has led to diminishing returns for developing effective new clinical candidates.<sup>8–14</sup> In some instances, bacterial strains have emerged that are resistant to all contemporary antibacterials, as well as older, more toxic drugs that clinicians are reverting to in more

desperate situations (e.g. polymyxins).<sup>15, 16</sup> To counter the diminishing antibacterial pipeline, it is crucial that new antibacterial candidates are developed that function through unexploited biological pathways. Furthermore, of particular urgency is to identify new antibiotic candidates that are effective against Gram-negative bacteria, since their lipopolysaccharide (LPS) outer membranes and efficient efflux pumps make them highly impermeable and intrinsically resistant to many antibacterial agents.

Towards identifying antibacterial candidates that function through fundamentally new mechanisms of action, researchers have recently begun exploring the possibility of targeting molecular chaperones as antibacterial strategies.<sup>17–25</sup> A broad class of molecular chaperones consist of several families of heat shock proteins (HSPs) that are categorized by the relative molecular weights of their subunits: HSP100, HSP90, HSP70, HSP60, HSP40, and small molecular weight HSPs.<sup>26–31</sup> Together, these HSPs form an intricate intracellular network that maintains protein homeostasis by helping unfolded polypeptides to fold to their native states, or targeting them for degradation when misfolding occurs. Our lab is focused on targeting the HSP60 class of molecular chaperones, known as GroEL in bacteria, as a mechanistically unique antibiotic strategy. As all bacteria contain at least one GroEL homolog that is essential under all conditions, this class of molecular chaperones represents a potential antibacterial target with broad spectrum applicability.<sup>29, 32–42</sup>

GroEL is comprised of two homo-heptameric rings that stack back-to-back with one another.<sup>43–54</sup> The 800 kDa *bis*-toroidal GroEL oligomer functions in conjunction with a 70 kDa homo-heptameric co-chaperone, called GroES, to fold substrate polypeptides in an ATP-dependent manner. The GroEL/ES-mediated folding cycle is initiated when ATP and an unfolded polypeptide bind to a GroEL *cis*-ring. The positively cooperative binding of ATP to each of the seven GroEL subunits powers a conformational shift of the GroEL apical domains upwards, allowing them to engage with the GroES co-chaperone lid. Binding of GroES causes a greater conformational movement of the GroEL apical domains that releases the bound polypeptide substrate into the now enclosed GroEL/ES *cis*-chamber. The polypeptide is then allowed to try and refold on its own, sequestered from the outside cytoplasmic milieu, with ATP hydrolysis (~5–10 s) acting as the timing mechanism. ATP hydrolysis in the *cis*-ring sends an allosteric signal for ATP and another unfolded polypeptide substrate to then bind to the GroEL *trans*-ring. This initiates the release of the GroES lid from the *cis*-ring, along with the substrate protein. If the substrate protein has not achieved its native state, it can re-attempt the folding process or be targeted for degradation.

In 2014, we reported a study that identified 235 GroEL/ES inhibitors from a high-throughput screen of 700,000 compounds.<sup>55</sup> Subsequent screening and analog derivatization of two hit-to-lead series – based on *bis*-sulfonamido-2-phenylbenzoxazole (**BSP**) and salicylanilide (**SCA**) scaffolds (Figure 1) – identified lead compounds that potently inhibited the proliferation of *E. faecium* and *S. aureus* bacteria (both Gram-positive), but that were largely ineffective against *E. coli* and the *KAPE* Gram-negative bacteria.<sup>56–59</sup> However, from our initial antibacterial testing, compound **1** stood out as another hit inhibitor of interest.<sup>57</sup> Despite being only a moderate GroEL/ES inhibitor, compound **1** exhibited weak to moderate antibacterial efficacy against *Bacillus subtilis*, methicillin-resistant *S. aureus*, *K. pneumoniae*, *A. baumannii*, and SM101 *E. coli* (which have a temperature sensitive protein in the LPS

biosynthetic pathway making the bacteria more permeable to drugs at non-permissive temperatures).<sup>60, 61</sup> Furthermore, the compound **1** scaffold resembles other known antibiotics that are active against Gram-negative bacteria. For instance, compound **1** shares its hydroxyquinoline substructure with nitroxoline, and its *bis*-cyclic-*N*-acylhydrazone core with nitrofurans-based antibiotics such as nifuroxazide and nitrofurantoin (Figure 1). While these drugs are primarily used to treat urinary tract infections, they also exhibit antibiotic effects against a range of pathogens including the *ESKAPE* bacteria.<sup>62–68</sup>

Based on the similarities of compound **1** with nitroxoline, nifuroxazide, and nitrofurantoin, we developed a library of analogs that probed the structure-activity relationships (SAR) of the cyclic/aryl substructures on both the right and left-hand sides of the *N*-acylhydrazone linker (Scheme 1). The right-hand substructure of these analogs contained either a hydroxyquinoline group (mimicking **1** and nitroxoline) or a nitrofurans group (mimicking nifuroxazide and nitrofurantoin), generating two distinct series of compounds. For each series, 15 left-side groups were assessed that contained a diverse range of substructures, including some that we have found effective with other GroEL/ES inhibitor scaffolds that have shown antibacterial properties (e.g. thiophenes, 2-chlorothiophenes, and aryl-sulfonamides).<sup>56–58, 71</sup> These analogs were tested in a panel of *in vitro* assays for bacterial proliferation inhibition, GroEL/ES inhibition (both substrate folding and ATPase functions), human cell cytotoxicity, and bacterial resistance towards lead analogs. The results from testing analogs in this panel of biochemical and cell-based experiments are presented herein, with a discussion on SAR and the potential of these series as GroEL/ES-targeting antibacterial candidates.

## 2. RESULTS AND DISCUSSION

### 2.1 Conceptualizing and developing the hydroxyquinoline and nitrofurans-containing series of compound **1** analogs.

Owing to their similarity to the known antibacterials nitroxoline, nifuroxazide, and nitrofurantoin, we investigated two primary series of compound **1** analogs that also bore hydroxyquinoline and nitrofurans substructures (Scheme 1). For each series, 15 left-side groups were assessed that contain a diverse range of substructures, including some that we have found effective with other GroEL/ES inhibitor scaffolds that have shown antibacterial properties (e.g. thiophenes, 2-chlorothiophenes, and aryl-sulfonamides).<sup>56–58, 71</sup> A third group of analogs (**29–42**) was also investigated to determine which parts of the hydroxyquinoline and nitrofurans aryls were required for inhibitor potency in the respective assays (refer to Tables S1C and S2C in the Supporting Information for the structures of compounds **29–42**).

Analogues were all synthesized through a one-step coupling reaction between the respective aryl-aldehydes and *N*-acylhydrazides in DMSO, with HCl as a catalyst.<sup>69, 70</sup> After stirring overnight at room temperature, the final *N*-acylhydrazone products were precipitated through the addition of water, and the solids were filtered, rinsed, and dried *in vacuo* (synthetic yields ranged from 46–99%). Where necessary, compounds were further purified via normal and/or reverse-phase chromatography. Synthesized analogs were analyzed by RP-HPLC for purity and LC-MS and <sup>1</sup>H-NMR for structural confirmation (complete

characterization data can be found in the Supporting Information). While all compounds were found to be >95% pure using two distinct sets of RP-HPLC conditions, for some analogs (**3**, **4**, **6**, **9**, **10**, **17**, **23**), we noticed a splitting of peaks in the <sup>1</sup>H-NMR spectra. This phenomenon has previously been studied by others and reported as resulting from hindered rotation around the amide bond, providing rotational isomers (rotamers).<sup>72, 73</sup> Thus, we believe that the purity of these compounds is consistent with HPLC results showing >95% purity.

## 2.2 Evaluating analogs for inhibiting the growth of *E. coli* and the *ESKAPE* bacteria.

Analogs were initially tested for antibacterial efficacy against representative strains of antibiotic-sensitive *E. coli* and the *ESKAPE* bacteria (refer to the Materials & Methods section for strain and vendor information for the respective bacteria). To determine compound efficacy, bacterial proliferation assays were carried out in liquid media culture supplemented with physiological concentrations of free calcium and magnesium cations.<sup>74</sup> For these assays, bacterial cultures (OD<sub>600</sub> = 0.01) were exposed to test compounds in 8-point, 3-fold dilution series (100 μM to 46 nM concentration range), in 384-well plates. After addition of compounds to cultures, the plates were sealed with Breathe-Easy gas permeable membranes and allowed to grow to mid-log phase (OD<sub>600</sub> ~0.4–0.6) – to examine inhibition against actively-replicating bacteria – whereupon final OD<sub>600</sub> readings were taken to assess for bacterial growth and inhibition. An in-depth protocol for this common set of proliferation assays is provided in the Supporting Information, and calculated EC<sub>50</sub> values are reported in Tables 1 and S2. For easier visualization of results, tables are heat-mapped according to inhibitor potencies, with darker cells representing the most potent analogs, and lighter cells the least potent inhibitors.

Results from the bacterial proliferation assays indicated that the hydroxyquinoline analogs were largely ineffective against *E. coli* and the *ESKAPE* pathogens, although several weak inhibitors were identified. Prior to initiating this study, we had hypothesized that the weak metal-chelating properties of the hydroxyquinoline substructure might allow these inhibitors to act as siderophores that could be actively taken up into bacteria; however, the lack of efficacy in this series was perhaps not surprising as a previous study by Pelletier *et al.* had indicated that the antibacterial activity of nitroxoline was reduced upon cation supplementation.<sup>65, 75–78</sup> Despite this setback, we were excited to see that many of the nitrofurantoin-based analogs were much more effective at inhibiting bacterial growth. In particular, analogs **16–20**, **22–24**, and **26** were moderate to strong inhibitors of the Gram-positive *E. faecium* and *S. aureus* bacteria. For reasons that are not clear, and contrary to the GroEL/ES inhibition results (discussed below), the dimethylaniline (**21**) and bulkier sulfonamide-containing analogs (**25–28**) were less effective (or inactive) compared to the analogs with the smaller *N*-acylhydrazide substructures. Presumably these compounds suffered from efflux and/or poor permeability through the bacterial cell walls, since they were the most potent at inhibiting GroEL/ES and would thus be expected the most potent at killing bacteria if they achieved appreciably high intracellular concentrations, and presuming they were exhibiting on-target effects against GroEL/ES.

While antibacterial effects were limited against the Gram-negative *KAPE* bacteria, a few analogs (**16–21**) were potent against *E. coli*, with EC<sub>50</sub> values 11 μM. Compounds **16** and **17** were more potent than nitroxoline, nifuroxazide, and nitrofurantoin against *E. coli* (EC<sub>50</sub> values <1 μM), and were even moderate inhibitors of *K. pneumoniae*. These were significant findings as our previous studies failed to identify lead analogs with such high efficacies against *E. coli* or any of the Gram-negative *KAPE* bacteria.<sup>56–58</sup> As evidenced by the results of compound **39** (Table S2C), which has an unsubstituted furan ring, the nitro group was essential for antibacterial effects. This is putatively because nitrofurans are activated to reactive metabolites by nitroreductases in bacteria, which we discuss further below.<sup>79–83</sup> Additionally, the hydroxyquinoline and nitrofurans were potent inhibitors of nearly all the bacteria (excluding *P. aeruginosa*), yet the *N*-acylhydrazone analogs were largely ineffective against the *KAPE* bacteria, supporting our belief that the linkers were not hydrolyzing and releasing the starting materials. Therefore, inhibitor potencies likely owed to the final products themselves, or their metabolites in the case of the nitrofurans series.

### 2.3 Evaluating analogs for inhibiting GroEL/ES-mediated substrate refolding functions.

Since we identified several analogs that potently inhibited the growth of both Gram-positive and Gram-negative bacteria, we next evaluated their abilities to inhibit *E. coli* GroEL/ES-mediated substrate folding functions *in vitro*. We first evaluated all test compounds in our standard GroEL/ES-mediated refolding assays that employ either malate dehydrogenase (MDH) or rhodanese (Rho) as the denatured substrate reporter enzymes (detailed descriptions of the assay protocols are presented in the Supporting Information).<sup>56–59, 71, 84</sup> When denatured, these enzymes are efficiently folded by GroEL/ES in the absence of inhibitors, and thus act as reporters to determine the degree of inhibition against the bacterial chaperonin system. Inhibition was examined in the presence of these two orthogonal substrates in order to support that inhibitors were acting against the chaperonin system. We further counter-screened for inhibition of native MDH and Rho – where test compounds were added after the denatured MDH and Rho substrate enzymes were completely refolded by GroEL/ES – to identify false positives that may simply act by inhibiting the enzymatic reporter reactions of the coupled refolding assays. We have found that these series of four biochemical assays are highly effective at eliminating false-positives as compounds rarely inhibit both reporter enzymes since their enzymatic read-outs are so different from one another. IC<sub>50</sub> results for all compounds tested in these four assays are presented in Tables S1A – S1C in the Supporting Information.

Unfortunately, we found that the nitrofurans were only weak to moderate GroEL/ES inhibitors despite being the most potent at inhibiting bacterial growth (see the white diamond symbols in the correlation plots of Figure 2A). Conversely, the hydroxyquinoline analogs (black circles in Figure 2A) were much stronger GroEL/ES inhibitors, although they were largely inactive against bacteria. While the hydroxyquinolines were slightly more potent in the GroEL/ES-mediated dRho compared to dMDH refolding assays (Figure 2A), this was likely because several of them had the coupled effects of also being weak inhibitors of the native Rho reporter reaction (Figure 2B); however, no compounds inhibited native MDH, supporting that the GroEL/ES inhibitors were not false-positives. Analogs **29–38**,

where the various parts of the hydroxyquinoline substructure were pared away, were largely inactive in all biochemical assays, indicating the necessity for the complete hydroxyquinoline moiety for inhibition. As mentioned in the previous section, the dimethylaniline-nitrofurans (**21**) and bulkier sulfonamide-containing analogs (**12–15** and **25–28**) were generally the most potent GroEL/ES inhibitors, yet the least effective or inactive against bacteria, suggesting they were unable to penetrate bacteria or were quickly effluxed out – otherwise they would have been expected to exhibit stronger antibacterial effects. Although, this is presuming that the antibacterial effects of these analogs was from on-target inhibition of GroEL/ES, which remains to be proven.

#### 2.4 Evaluating analogs for inhibiting GroEL/ES-mediated substrate refolding functions in the presence of the *E. coli* NfsB type-1 nitroreductase.

That none of the nitrofurans were found to be potent GroEL/ES inhibitors is complicated by the fact that nitrofurans-based antibiotics are known to act as prodrugs *in vivo* – they require metabolism by bacterial nitroreductases to generate reactive metabolites that are associated with their antibacterial effects.<sup>79–83</sup> However, our standard GroEL/ES-mediated refolding assays and native substrate reporter counter-screens were conducted without nitroreductases present. This emphasized the need to re-examine analogs in modified refolding and native reporter activity assays that included a nitroreductase enzyme to activate the nitrofurans *in situ*, which would be more representative of the bacterial intracellular environment. As an initial test to see whether or not the activated nitrofurans metabolites would be more potent GroEL/ES inhibitors, we purchased the *E. coli* NfsB type 1 nitroreductase and modified our standard GroEL/ES-dMDH refolding and native MDH counter-screens to generate the reactive metabolites *in situ* (detailed protocols for these assays are presented in the Materials & Methods section). We have reported IC<sub>50</sub> results from these assays in Table S1A – S1C in the Supporting Information, and graphically in the correlation plot of Figure 2C, where IC<sub>50</sub> values are compared between compounds tested in the GroEL/ES-dMDH refolding assay with and without the *E. coli* NfsB nitroreductase.

We were excited to see that in the presence of *E. coli* NfsB, the nitrofurans exhibited dramatically increased inhibition of GroEL/ES refolding functions. The IC<sub>50</sub> values for the hydroxyquinoline (**1–15**) and other analogs without nitro groups (e.g. **29–42**) were nearly identical in the presence and absence of NfsB, supporting that increased inhibition was dependent on modification of the nitrofurans moiety and not other effects on the overall compound scaffold or from NfsB itself. Furthermore, the nitrofurans metabolites were inactive in the native MDH reporter counter-screen, indicating that increased inhibition was obtained through selectively targeting the GroEL/ES-mediated refolding cycle. While the degree of potency shift varied between analogs, ten shifted to IC<sub>50</sub> values < 11 μM. As points of comparison, the most potent nitrofurans analog in the absence of NfsB had an IC<sub>50</sub> = 26 μM (analog **21**), with six being completely inactive (IC<sub>50</sub> > 100 μM). Significant potency shifts were observed for the most effective antibacterials (**16–20**), showing that some of the strongest antibacterial compounds were also strong GroEL/ES inhibitors when activated by a nitroreductase enzyme. While activated nitrofurazone and nitrofurantoin were only weak to moderate GroEL/ES inhibitors in this new assay, this may not be surprising as they are

reported in the literature to be preferentially activated by the other *E. coli* type 1 nitroreductase, NfsA.<sup>80, 82, 85</sup>

While we observed a general trend whereby the more potent that nitrofurans were in the *in situ* NfsB-GroEL/ES-dMDH refolding assay, the more potent they were at inhibiting *S. aureus* proliferation (Figure 3B), we are guarded as to whether or not inhibitors were potentially functioning on-target in bacteria. We note the limitations in such an overly simplistic comparison since we had tested such a small set of analogs, and only tested them in the presence of *E. coli* NfsB. As the different nitrofurans would be expected to exhibit varying SAR for activation by NfsA and NfsB, it will be important to test inhibitors in the presence of both nitroreductases to gain a more complete picture of how they could be functioning in bacteria. We are in the process of cloning and expressing *E. coli* *nfsA* and *nfsB* and developing an expanded panel of nitrofurans-based analogs to study inhibitor mechanisms in greater detail. Furthermore, investigating the nitroreductases of the various *ESKAPE* bacteria could provide a stronger rationale for why these compounds were largely inactive against the *KAPE* Gram-negative strains. Another limitation was that we were using the *E. coli* GroEL/ES chaperonin system as a surrogate in our assays. While we anticipate inhibition results will translate to the chaperonin systems of the other *ESKAPE* bacteria owing to their high sequence similarities (between 55–95% amino acid identity between the chaperonins from *E. coli* and the *ESKAPE* bacteria), this still remains to be demonstrated. Thus, we are also in the process of generating recombinant versions of the respective *ESKAPE* bacteria GroEL and GroES proteins and will report on such inhibition results in the future.

## 2.5 Evaluating analogs for inhibiting GroEL-mediated ATPase activity.

Since many proteins use ATP for their biological functions, inhibiting GroEL/ES by competitively binding to the ATP sites could prove problematic for being able to selectively target the chaperonin system. Thus, we further tested analogs in a well-established GroEL ATPase assay that employed malachite green to monitor inorganic phosphate liberated as GroEL hydrolyzed ATP.<sup>55, 59, 84</sup> Briefly, a solution of GroEL was incubated with test compounds (8-point, 3-fold dilution series) and the assay was initiated by addition of ATP. After incubating for 45 minutes, the ATPase reaction was quenched by the addition of EDTA. Malachite green was then added to the assay to bind and detect free phosphates in solution (absorbance detection at  $\lambda=600$  nm). If analogs inhibited ATPase activity, then there would be no free phosphates for malachite green to bind, leading to minimal absorbance at 600 nm. The detailed procedure for this assay is presented in the Supporting Information. As indicated in Tables S1A to S1C in the Supporting Information, none of the analogs from either series inhibited GroEL by blocking ATP hydrolysis. Thus, we believe that these inhibitors bind to sites outside of the ATP pockets. We are pursuing and will report on studies to identify these unknown binding sites in the future. While these results alleviate concerns about non-selectively targeting other ATP-dependent proteins, we further assessed off-target effects through a more definitive approach by evaluating analog cytotoxicity in two human cell lines, discussed below.



## 2.6 Evaluating the cytotoxicity of analogs to human colon and small intestinal cells.

While in previous studies we have employed biochemical counter-screening with the human mitochondrial HSP60/10 chaperonin system, our accumulating results indicate that inhibiting HSP60/10 *in vitro* is a poor indicator of potential off-target toxicity to human cells.<sup>57–59, 84</sup> This is highlighted by the fact that we have identified many known drugs and natural products that are potent inhibitors of HSP60/10 biochemical function *in vitro*, yet exhibit little to no adverse effects in cells or animals. For instance, we found that suramin is a potent HSP60/10 inhibitor, yet it has been used safely for over 100 years as a first-line treatment for *Trypanosoma brucei* infections.<sup>59, 84</sup> In addition, as now identified in this study, bioactivation of nitrofurantoin by nitroreductase enzymes greatly increases the extent of inhibition against GroEL/ES refolding activity, and potentially human HSP60/10; however, this further complicates testing against HSP60/10 since human cells do not contain nitroreductases. Therefore, we feel the most appropriate initial assessment of potential *in vivo* toxicity is to test compounds for cytotoxicity to human cells in culture.

To assess for potential cytotoxic effects, compounds were tested in two Alamar Blue-based cell viability assays using human FHC colon and FHs 74 Int small intestinal cells. Briefly, we grew cells to ~80–90% confluency, then sub-cultured 1,500 cells per well (in 384-well plates) for 24 h in the absence of test compounds. Compounds were then added and the cultures were incubated for an additional 48 h, whereupon the Alamar Blue reporter reagents were added and well fluorescence was monitored over time. Alamar Blue contains resazurin (non-fluorescent), which is reduced to resorufin (highly fluorescent) in the presence of viable cells. A detailed protocol is presented in the Supporting Information, along with cell cytotoxicity CC<sub>50</sub> values in Tables S2A – S2C. As graphically presented in the Figure 4 correlation plots comparing bacterial proliferation EC<sub>50</sub> to human cell cytotoxicity CC<sub>50</sub> results, lead nitrofurantoin inhibitors (**16**, **17**, **20**, nitrofurantoin, and nifuroxazide) selectively inhibited *E. faecium*, *S. aureus*, and *E. coli* proliferation with low to no cytotoxicity to human cells (representative results are shown for human FHs 74 Int small intestine cells, but results are similar for FHC colon cells and are presented in Figure S1 in the Supporting Information). Intriguingly, the nitrofurantoin analogs were typically less toxic than their hydroxyquinoline counterparts, putatively because they would need to be metabolized to their active intermediates, yet human cells do not harbor nitroreductases.

## 2.7 Investigating the ability of *E. coli* to gain resistance to **17**, nifuroxazide, and nitrofurantoin.

As we discovered several nitrofurantoin-based analogs that selectively inhibited the growth of *E. faecium*, *S. aureus*, and *E. coli* with minimal toxicity to human cells, we next investigated how easy it would be for bacteria to generate resistance to a lead candidate. We examined the ability of *E. coli* to generate resistance to **17** (with nifuroxazide and nitrofurantoin as controls), since resistance to nitrofurantoin-based antibiotics has been well-characterized in this bacterium. While **17**, nifuroxazide, and nitrofurantoin were all potent inhibitors of *E. coli* proliferation, **17** was the most potent at inhibiting GroEL/ES in the presence of NfsB, and thus may exhibit greater on-target effects in bacteria. However, as discussed above, we do appreciate the limitations of not employing NfsA. To identify differences in the ability of *E. coli* to generate resistance to these three compounds with such distinct bioactivity profiles,

we employed a 12 day resistance assay as we previously reported for our salicylanilide lead candidate *S. aureus* inhibitors (a detailed protocol is included in the Supporting Information).<sup>58</sup> Briefly, a dilute culture of *E. coli* ( $OD_{600} = 0.01$ ) was grown in the presence of inhibitors for 24 h (tested in dose-response in duplicates), then  $EC_{50}$  results were determined from the  $OD_{600}$  readings of the wells. Over the course of 12 days, we sequentially sub-cultured bacteria from the respective wells with the highest concentration of inhibitors where bacteria grew to an  $OD_{600} > 0.2$ , monitoring for increases in  $EC_{50}$  values over time.

While we found that nifuroxazide and nitrofurantoin were initially more potent than **17** (Figure 5), *E. coli* quickly developed intermediate resistance (within 3–5 days) such that all three inhibitors were nearly equipotent. This initial resistance was putatively through mutations affecting NfsA function, as has been previously reported by others.<sup>80</sup> That  $EC_{50}$  values then somewhat plateaued in the 20–40  $\mu\text{M}$  range is consistent with NfsB still being able to metabolize the nitrofuranyl moieties and maintain efficacy, albeit at a reduced capacity.  $EC_{50}$  values continued to slowly increase over time for all three compounds, with a particular jump in resistance seen for the second set of replicates for nitrofurantoin and nifuroxazide to a lesser extent, but not for **17**. Thus, inhibitors that are preferentially activated by NfsB, as may be the case for **17**, might be more effective drug candidates with respect to combatting the emergence of drug resistant strains. We are cautious in over-interpreting these results since the experiment was only conducted in duplicate for three analogs, and further studies are warranted.

We next confirmed that the resistance generated by the replicate *E. coli* strains was irreversible (i.e. putatively through permanent mutations of NfsA and NfsB as previously reported by others) as opposed to transient means (i.e. by up-regulating efflux pumps). To accomplish this, we sub-cultured single colonies obtained from the replicate samples where the bacteria exhibited the greatest degree of resistance to test compounds (day 12 samples for all compound replicates, except replicate 2 for nitrofurantoin, which was taken at day 10), for  $4 \times 12$  h serial passages in fresh media without any test compounds present. We then performed another 24 h follow-up proliferation assay to determine  $EC_{50}$  values (dose-response curves are presented for nifuroxazide, nitrofurantoin, and **17** in Figures 6 and S2 in the Supporting Information). Results indicated that these subsequently-cultured bacterial strains were still resistant to each of the respective inhibitors they were generated from, supporting that resistance mechanisms were permanent. As previous studies by others have extensively characterized mutations affecting NfsA and NfsB that *E. coli* acquire to generate resistance against nitrofuranyl antibiotics, we did not perform genotyping to further characterize the specific resistance mechanisms for these strains, as they were likely the same.<sup>80</sup>

Since nifuroxazide, nitrofurantoin, and **17** displayed different inhibition and resistance profiles, we next examined if the respective resistant strains were cross-resistant with each of the other inhibitors. Intriguingly, while the replicate strains that were initially resistant to nifuroxazide were cross-resistant to both nitrofurantoin and **17** (Figures 7A and S3A in the Supporting Information), the nitrofurantoin-resistant strains were still sensitive to nifuroxazide and **17** (Figures 7B and S3B), and the **17**-resistant strains were susceptible to

nifuroxazide, but not nitrofurantoin (Figures 7C and S3C). Thus, it is evident that strains that have generated resistance to one analog are not necessarily cross-resistant to other analogs. Further studies are warranted to see if combination therapy with two or more inhibitor analogs might be synergistic and prevent or prolong the emergence of resistant strains.

### 3. CONCLUSIONS

In a previous high-throughput screen, we identified compound **1** as a moderate GroEL/ES inhibitor with weak to moderate antibacterial efficacy against *B. subtilis*, MRSA, *K. pneumoniae*, *A. baumannii*, and SM101 *E. coli* (which has a temperature sensitive LPS biosynthetic pathway). Intriguingly, key substructures of compound **1** resembled those of nitroxoline (i.e. shared hydroxyquinoline moiety) and nitrofurans-based antibacterials such as nifuroxazide and nitrofurantoin (i.e. shared *bis*-cyclic-*N*-acylhydrazone cores). Thus, we developed two parallel series of hydroxyquinoline and nitrofurans-bearing compound **1** analogs in an effort to increase inhibitor potency against GroEL/ES and *E. coli* and the *ESKAPE* bacteria, while reducing cytotoxicity to human cells (a compilation of assay results for nitrofurantoin, nifuroxazide, and lead analogs **16–21** is presented in Table 2). Initially, only the hydroxyquinoline series was found to contain potent GroEL/ES inhibitors in our traditional GroEL/ES-mediated substrate refolding assays; however, subsequent testing in the presence of *E. coli* NfsB indicated that the nitrofurans act as pro-drugs and their reactive metabolites can be potent GroEL/ES inhibitors. Lead nitrofurans were potent inhibitors of *E. faecium*, *S. aureus*, and *E. coli* proliferation and exhibited minimal cytotoxicity to human FHC colon and FHs 74 Int small intestinal cells. While *E. coli* were able to generate varying degrees of irreversible resistance to nifuroxazide, nitrofurantoin, and lead analog **17** (putatively through mutations in NfsA and NfsB), clones were not necessarily cross-resistant to the other inhibitors. This finding may indicate diverging mechanisms of activation and/or targets for structurally distinct inhibitors, suggesting that combination therapy could prove synergistic and delay the onset of bacterial resistance.

Perhaps most importantly, the present study has identified a new target for a large class of clinical drugs whose mode of action is ambiguous. While we had previously identified that GroEL/ES affects similar proteins and pathways as nitrofurans-containing drugs – e.g. perturbing protein synthesis, aerobic energy metabolism, DNA synthesis, RNA synthesis, and cell wall synthesis – further studies are warranted to elucidate whether targeting GroEL/ES may be a driver of their bioactivities.<sup>33</sup> While we note the limitations of having evaluated compounds in biochemical assays using only the *E. coli* GroEL/ES chaperonin system and NfsB as surrogates, a more thorough analysis against the various chaperonin systems and nitroreductases from *E. coli* and the *ESKAPE* bacteria is a monumental undertaking beyond the scope of the present study. However, having identified this new chaperonin-targeting pro-drug inhibition mechanism for nitrofurans-containing drugs, this study provides the impetus for us to undertake such an arduous task. We will report on our ongoing findings in future studies.

## 4. MATERIALS & METHODS

### General Synthetic Methods.

Unless otherwise stated, all chemicals were purchased from commercial suppliers and used without further purification. Reaction progress was monitored by thin-layer chromatography on silica gel 60 F254 coated glass plates (EM Sciences). Flash chromatography was performed using a Biotage Isolera One flash chromatography system and eluting through Biotage KP-Sil Zip or Snap silica gel columns for normal-phase separations (hexanes:EtOAc gradients), or Snap KP-C18-HS columns for reverse-phase separations (H<sub>2</sub>O:MeOH gradients). Reverse-phase high-performance liquid chromatography (RP-HPLC) was performed using a Waters 1525 binary pump, 2489 tunable UV/Vis detector (254 and 280 nm detection), and 2707 autosampler. For preparatory HPLC purification, samples were chromatographically separated using a Waters XSelect CSH C18 OBD prep column (part number 186005422, 130 Å pore size, 5 µm particle size, 19×150 mm), eluting with a H<sub>2</sub>O:CH<sub>3</sub>CN gradient solvent system. Linear gradients were run from either 100:0, 80:20, or 60:40 A:B to 0:100 A:B (A = 95:5 H<sub>2</sub>O:CH<sub>3</sub>CN, 0.05% TFA; B = 5:95 H<sub>2</sub>O:CH<sub>3</sub>CN, 0.05% TFA). Products from normal-phase separations were concentrated directly, and reverse-phase separations were concentrated, diluted with H<sub>2</sub>O, frozen, and lyophilized. For primary compound purity analyses (HPLC-1), samples were chromatographically separated using a Waters XSelect CSH C18 column (part number 186005282, 130 Å pore size, 5 µm particle size, 3.0×150 mm), eluting with the above H<sub>2</sub>O:CH<sub>3</sub>CN gradient solvent systems. For secondary purity analyses (HPLC-2) of final test compounds, samples were chromatographically separated using a Waters XBridge C18 column (part number 186003132, 130 Å pore size, 5.0 µm particle size, 3.0×100 mm), eluting with a H<sub>2</sub>O:MeOH gradient solvent system. Linear gradients were run from either 100:0, 80:20, 60:40, or 20:80 A:B to 0:100 A:B (A = 95:5 H<sub>2</sub>O:MeOH, 0.05% TFA; B = 5:95 H<sub>2</sub>O:MeOH, 0.05% TFA). Test compounds were found to be >95% in purity from both RP-HPLC analyses. Mass spectrometry data were collected using either Agilent LC 1200-MS 6130 or Agilent LC 1290-MS 6545 Q-TOF analytical LC-MS instruments at the IU Chemical Genomics Core Facility (CGCF). <sup>1</sup>H-NMR spectra were recorded on a Bruker 300 MHz spectrometer at the IU CGCF. Chemical shifts are reported in parts per million and calibrated to the *d*<sub>6</sub>-DMSO solvent peaks at 2.50 ppm. A representative synthesis of all analogs is presented below in the context of compound **1**. <sup>1</sup>H-NMR, MS, and HPLC characterization data are presented in the Supporting Information for the remaining analogs.

**1: N<sup>2</sup>-((8-hydroxyquinolin-5-yl)methylene)-4-methoxybenzohydrazide.**—To a stirring mixture of 4-methoxybenzoic acid hydrazide (668 mg, 4.02 mmol) and 8-hydroxyquinoline-5-carbaldehyde (583 mg, 3.37 mmol) was added a catalytic amount of HCl (0.09 mL of a 4N solution in 1,4-dioxane, 0.36 mmol) in 10 mL of DMSO, then the reaction was left to stir at rt overnight. The following day, the reaction was diluted with distilled water and the precipitate was filtered, rinsed with distilled water, collected, and dried to afford **1** as a yellow solid (1.07 g, 99% yield). <sup>1</sup>H-NMR (300 MHz, *d*<sub>6</sub>-DMSO) δ 11.70 (s, 1H), 10.44 (br s, 1H), 9.61 (d, *J* = 8.6 Hz, 1H), 8.94 (d, *J* = 2.8 Hz, 1H), 8.81 (s, 1H), 7.90–8.01 (m, 2H), 7.68–7.82 (m, 2H), 7.17 (d, *J* = 8.1 Hz, 1H), 7.04–7.13 (m, 2H),

3.85 (s, 3H); MS (ESI) C<sub>18</sub>H<sub>16</sub>N<sub>3</sub>O<sub>3</sub> [MH]<sup>+</sup> *m/z* expected = 322.1, observed = 322.1; HPLC-1 = 99%; HPLC-2 = 99%.

### General materials and methods for biochemical & cell-based experiments.

The bacterial proliferation assays employed the following bacterial strains: NEB 5-alpha *Escherichia coli* (a derivative of DH5α *E. coli*, New England Biolabs #C2987H); *Enterococcus faecium* - (Orla-Jensen) Schleifer and Kilpper-Balz strain NCTC 7171 (ATCC #19434); *Staphylococcus aureus* - Rosenbranch strain Seattle 1945 (ATCC #25923); *Klebsiella pneumoniae* - (Schroeter) Trevisan strain NCTC 9633 (ATCC #13883); *Acinetobacter baumannii* - Bouvet and Grimont strain 2208 (ATCC 19606); *Pseudomonas aeruginosa* - (Schroeter) Migula strain NCTC 10332 (ATCC #10145); *Enterobacter cloacae* - *E. cloacae*, subsp. *cloacae* (Jordan) Hormaeche and Edwards strain CDC 442-68 (ATCC #13047). For protein expression and purification, NEB 5-alpha and BL21 (DE3) *E. coli* cells were purchased from New England Biolabs, and Rosetta™ 2 (DE3) *E. coli* cells were purchased from EMD Millipore. The human cell viability assays used FHC colon cells (CRL-1831) and FHs 74 Int small intestine cells (CCL-241) obtained from the ATCC. Ampicillin was used at a concentration of 50 µg/mL, when appropriate.

### Expression and purification of *E. coli* GroEL and GroES proteins.

*E. coli* GroEL and GroES were expressed and purified as previously reported.<sup>55-59, 71, 84, 86, 87</sup> Detailed protocols for these protein purifications are presented in the Supporting Information.

### Evaluating compounds for inhibition in the GroEL/ES-mediated dMDH refolding assay.

All compounds were evaluated for inhibiting *E. coli* GroEL/ES-mediated refolding of the denatured MDH reporter enzyme as per our previously reported procedure.<sup>55-59, 71, 84</sup> A detailed protocol for this assay is presented in the Supporting Information. Results presented represent the averages of IC<sub>50</sub> values obtained from at least four replicates.

### Counter-screening compounds for inhibition of native MDH enzymatic activity.

All compounds were counter-screened for inhibiting the enzymatic activity of the native MDH reporter enzyme as per our previously reported procedure<sup>55-59, 71, 84</sup> A detailed protocol for this assay is presented in the Supporting Information. Results presented represent the averages of IC<sub>50</sub> values obtained from at least five replicates.

### Evaluating compounds for inhibition in the GroEL/ES-mediated dMDH refolding assay and native MDH activity counter-screen in the presence of *E. coli* NfsB nitroreductase.

These assays were performed nearly identically to those mentioned above, but with a couple distinct modifications (detailed procedures are presented in the Supporting Information). For both assays, 10 µg/mL of the *E. coli* NfsB nitroreductase enzyme (Sigma product #N9284) was added to the initial GroEL/ES-dMDH solution. For the GroEL/ES-dMDH refolding assay, after stamping with compounds, 10 µL of a 2.4 mM NADH solution was added, followed by a 10 minute incubation period at 37°C to bioactivate the nitrofurans. The remainder of the assay was conducted as in our standard protocol where no NfsB

nitroreductase was present. With the extra 10  $\mu\text{L}$  volume from the NADH addition, this made the compound concentrations during the refolding cycle part of the assay range from 83  $\mu\text{M}$  to 38 nM (3-fold dilution series). For the native MDH activity counter-screen in the presence of *E. coli* NfsB nitroreductase, the assay was performed as described above for the GroEL/ES-dMDH refolding assay with NfsB; however, compound addition to the assay plates was conducted after the EDTA quench step, followed by a 10 minute incubation period at 37°C to bioactivate the nitrofurans. With the extra 10  $\mu\text{L}$  volume from the NADH addition, this made the compound concentrations during the enzymatic reporter part of the assay range from 56  $\mu\text{M}$  to 25 nM (3-fold dilution series). IC<sub>50</sub> values for the test compounds were obtained by plotting the % inhibition results in GraphPad Prism and analyzing by non-linear regression using the log(inhibitor) vs. response (variable slope) equation. Results presented represent the averages of IC<sub>50</sub> values obtained from at least four replicates in each assay.

#### **Evaluating compounds for inhibition in the GroEL/ES-mediated dRho refolding assay.**

All compounds were evaluated for inhibiting *E. coli* GroEL/ES-mediated refolding of the denatured Rho reporter enzyme as per our previously reported procedure.<sup>56-59, 71, 84</sup> A detailed protocol for this assay is presented in the Supporting Information. Results presented represent the averages of IC<sub>50</sub> values obtained from at least four replicates.

#### **Counter-screening compounds for inhibition of native rhodanese enzymatic activity.**

All compounds were counter-screened for inhibiting the enzymatic activity of the native Rho reporter enzyme as per our previously reported procedure.<sup>56-59, 71, 84</sup> A detailed protocol for this assay is presented in the Supporting Information. Results presented represent the averages of IC<sub>50</sub> values obtained from at least four replicates.

#### **Evaluating compounds for inhibition in the GroEL-mediated ATPase assay.**

All compounds were evaluated for inhibiting *E. coli* GroEL-mediated ATPase activity as per our previously reported procedure although employing only GroEL in solution and not containing GroES or denatured MDH.<sup>55, 59, 84</sup> A detailed protocol for this assay is presented in the Supporting Information. Results presented represent the averages of IC<sub>50</sub> values obtained from at least four replicates.

#### **Evaluating compounds for inhibition of bacterial cell proliferation.**

All compounds were evaluated for inhibiting the proliferation of *E. coli* and each of the *ESKAPE* bacteria as per previously reported procedures.<sup>56, 58</sup> A detailed protocol for the general bacterial growth assay used for each bacterium is presented in the Supporting Information. Results presented represent the averages of EC<sub>50</sub> values obtained from at least four replicates.

#### **Evaluating compound effects on the viability of human colon and small intestine cells.**

All compounds were evaluated for cytotoxicity to human colon (FHC) and small intestine (FHs 74 Int) cells using an Alamar Blue-based viability assay analogous to previously reported procedures.<sup>56-59, 71</sup> A detailed protocol for the general cell viability assay used for

both cell lines is presented in the Supporting Information. Results presented represent the averages of CC<sub>50</sub> values obtained from at least four replicates for the FHC and three replicates for the FHs 74 Int cell lines.

### Evaluating the ability of *E. coli* to generate resistance to lead inhibitors.

To identify potential resistance toward nifuroxazide, nitrofurantoin, and lead inhibitor **17**, a liquid culture, 12-day serial passage assay was employed as per previously reported procedures, and using the NEB 5-alpha *E. coli*.<sup>4, 56, 58, 88</sup> A detailed protocol for this assay is presented in the Supporting Information.

### Control compounds, calculation of IC<sub>50</sub> / EC<sub>50</sub> / CC<sub>50</sub> values, and statistical considerations.

For all assays, DMSO was used as negative control and a panel of our previously discovered and reported chaperonin inhibitors were used as positive controls: e.g. compounds **8**, **9**, and **18** from Johnson *et. al* 2014 and Abdeen *et. al* 2016;<sup>55, 57</sup> suramin and compound **2h-p** from Abdeen *et. al* 2016;<sup>59</sup> compounds **20R**, **20L**, and **28R** from Abdeen *et. al* 2018;<sup>56</sup> and closantel and rafoxanide from Kunkle *et. al* 2018.<sup>58</sup> Bacterial proliferation assays also included antibiotic controls such as vancomycin, daptomycin, and rifampicin.<sup>56, 58</sup> All IC<sub>50</sub> / EC<sub>50</sub> / CC<sub>50</sub> results reported are averages of values determined from individual dose-response curves in assay replicates as follows: 1) individual I/E/CC<sub>50</sub> values from assay replicates were first log-transformed and the average log(I/E/CC<sub>50</sub>) values and standard deviations (SD) calculated; 2) replicate log(I/E/CC<sub>50</sub>) values were evaluated for outliers using the ROUT method in GraphPad Prism (Q of 10%); and 3) average I/E/CC<sub>50</sub> values were then back-calculated from the average log(I/E/CC<sub>50</sub>) values. To compare log(IC<sub>50</sub>) values between different assays, two-tailed Spearman correlation analyses were performed using GraphPad Prism (95% confidence level). For compounds where log(I/E/CC<sub>50</sub>) values were greater than the maximum compound concentrations tested (i.e. >1.75, >1.80, >1.92, >2.00, and >2.40 – or >56, >63, >83, >100, and >250 μM, respectively), results were represented as 0.1 log units higher than the maximum concentrations tested (i.e. 1.85, 1.90, 2.02, 2.10, and 2.50 – or 71, 79, 105, 126, and 316 μM, respectively) so as not to overly bias results because of the unavailability of definitive values for inactive compounds.

### Supplementary Material

Refer to Web version on PubMed Central for supplementary material.

### ACKNOWLEDGMENTS

The authors declare no competing financial interests. Research reported in this publication was supported by the National Institute of General Medical Sciences (NIGMS) of the National Institutes of Health (NIH) under Award Number R01GM120350. QQH and YP additionally acknowledge support by NIH grants 5R01GM111639 and 5R01GM115844. The content is solely the responsibility of the authors and does not necessarily represent the official views of the NIH. This work was also supported in part by startup funds from the IU School of Medicine (SMJ) and the University of Arizona (EC).

### ABBREVIATIONS:

**HSP** Heat shock protein

<b>BSP</b>	<i>bis</i> -sulfonamido-2-phenylbenzoxazole
<b>SCA</b>	salicylanilide
<b>HQ</b>	hydroxyquinoline series
<b>NF</b>	nitrofurans series
<b>MDH</b>	malate dehydrogenase
<b>Rho</b>	rhodanese
<b>Nfz</b>	nifuroxazide
<b>Nft</b>	nitrofurantoin
<b>Nox</b>	nitroxoline
<b>NR</b>	nitroreductase

## 7. REFERENCES

1. WHO. No time to wait: Securing the future from drug-resistant infections; World Health Organization: 2019; p 28.
2. Centers for Disease Control and Prevention. Antibiotic resistance threats in the United States, 2019. Centers for Disease Control and Prevention: Atlanta, Georgia, USA, 2019; p 148.
3. Pendleton JN; Gorman SP; Gilmore BF Clinical relevance of the ESKAPE pathogens. *Expert Rev Anti-Infe* 2013, 11, 297–308.
4. Fleeman R; LaVoi TM; Santos RG; Morales A; Nefzi A; Welmaker GS; Medina-Franco JL; Giulianotti MA; Houghten RA; Shaw LN Combinatorial libraries as a tool for the discovery of novel, broad-spectrum antibacterial agents targeting the ESKAPE pathogens. *J. Med. Chem* 2015, 58, 3340–55. [PubMed: 25780985]
5. Karlowsky JA; Hoban DJ; Hackel MA; Lob SH; Sahm DF Antimicrobial susceptibility of Gram-negative ESKAPE pathogens isolated from hospitalized patients with intra-abdominal and urinary tract infections in Asia-Pacific countries: SMART 2013–2015. *J. Med. Microbiol* 2017, 66, 61–69. [PubMed: 28051952]
6. Rice LB Federal funding for the study of antimicrobial resistance in nosocomial pathogens: No ESKAPE. *J. Infect. Dis* 2008, 197, 1079–1081. [PubMed: 18419525]
7. Santajit S; Indrawattana N Mechanisms of antimicrobial resistance in ESKAPE pathogens. *Biomed. Res. Int* 2016, 2016, 2475067. [PubMed: 27274985]
8. Boucher HW; Talbot GH; Bradley JS; Edwards JE; Gilbert D; Rice LB; Scheld M; Spellberg B; Bartlett J Bad bugs, no drugs: No ESKAPE! An update from the Infectious Diseases Society of America. *Clin. Infect. Dis* 2009, 48, 1–12. [PubMed: 19035777]
9. Boucher H; Miller LG; Razonable RR Serious infections caused by methicillin-resistant *Staphylococcus aureus*. *Clin. Infect. Dis* 2010, 51 Suppl 2, S183–97. [PubMed: 20731576]
10. Boucher HW; Talbot GH; Benjamin DK; Bradley J; Guidos RJ; Jones RN; Murray BE; Bonomo RA; Gilbert D; Amer IDS 10 x '20 Progress-Development of New Drugs Active Against Gram-Negative Bacilli: An Update From the Infectious Diseases Society of America. *Clin Infect Dis* 2013, 56, 1685–1694. [PubMed: 23599308]
11. Lewis K Platforms for antibiotic discovery. *Nat. Rev. Drug Discov* 2013, 12, 371–87. [PubMed: 23629505]
12. World Health Organization. Treatment of Tuberculosis: Guidelines. 4th ed. ed.; World Health Organization: Geneva, Switzerland, 2010; p 160.
13. World Health Organization. Antibacterial agents in preclinical development: an open access database. World Health Organization: Geneva, Switzerland, 2019; p 20.

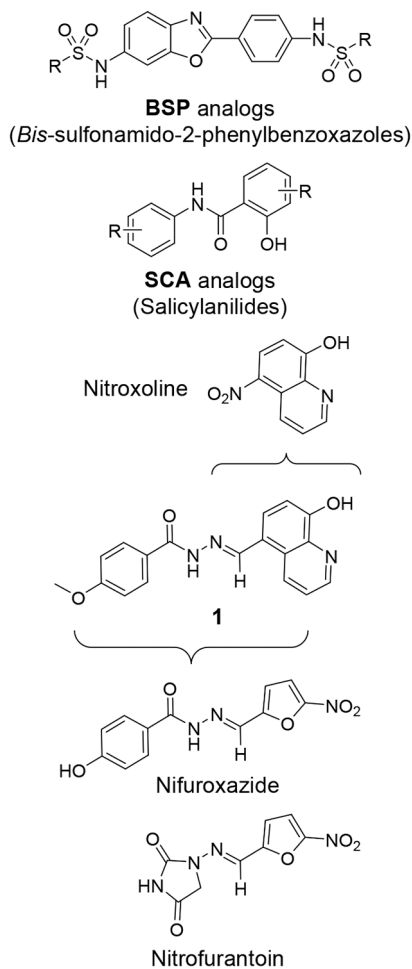


14. Theuretzbacher U; Outterson K; Engel A; Karlen A The global preclinical antibacterial pipeline. *Nat. Rev. Microbiol* 2020, 18, 275–285. [PubMed: 31745331]
15. Landman D; Georgescu C; Martin DA; Quale J Polymyxins revisited. *Clin. Microbiol. Rev* 2008, 21, 449–65. [PubMed: 18625681]
16. Poirel L; Jayol A; Nordmann P Polymyxins: Antibacterial Activity, Susceptibility Testing, and Resistance Mechanisms Encoded by Plasmids or Chromosomes. *Clin. Microbiol. Rev* 2017, 30, 557–596. [PubMed: 28275006]
17. Chiappori F; Fumian M; Milanesi L; Merelli I DnaK as antibiotic target: Hot spot residues analysis for differential inhibition of the bacterial protein in comparison with the human HSP70. *Plos One* 2015, 10, e0124563. [PubMed: 25905464]
18. Arita-Morioka K; Yamanaka K; Mizunoe Y; Ogura T; Sugimoto S Novel strategy for biofilm inhibition by using small molecules targeting molecular chaperone DnaK. *Antimicrob. Agents Chemother* 2015, 59, 633–41. [PubMed: 25403660]
19. Sass P; Josten M; Famulla K; Schiffer G; Sahl HG; Hamoen L; Brotz-Oesterhelt H Antibiotic acyldepsipeptides activate ClpP peptidase to degrade the cell division protein FtsZ. *Proc. Natl. Acad. Sci. U.S.A* 2011, 108, 17474–9. [PubMed: 21969594]
20. Evans CG; Chang L; Gestwicki JE Heat shock protein 70 (hsp70) as an emerging drug target. *J. Med. Chem* 2010, 53, 4585–602. [PubMed: 20334364]
21. Piper PW; Millson SH Spotlight on the microbes that produce heat shock protein 90-targeting antibiotics. *Open Biol.* 2012, 2, 120138. [PubMed: 23271830]
22. Neckers L; Tatu U Molecular Chaperones in Pathogen Virulence: Emerging New Targets for Therapy. *Cell Host Microbe* 2008, 4, 519–527. [PubMed: 19064253]
23. Kragol G; Lovas S; Varadi G; Condie BA; Hoffmann R; Otvos L Jr. The antibacterial peptide pyrrococidin inhibits the ATPase actions of DnaK and prevents chaperone-assisted protein folding. *Biochemistry* 2001, 40, 3016–26. [PubMed: 11258915]
24. Kumar A; Balbach J Targeting the molecular chaperone SlyD to inhibit bacterial growth with a small molecule. *Sci. Rep* 2017, 7, 42141. [PubMed: 28176839]
25. Lupoli TJ; Vaubourgeix J; Burns-Huang K; Gold B Targeting the Proteostasis Network for Mycobacterial Drug Discovery. *ACS Infect. Dis* 2018, 4, 478–498. [PubMed: 29465983]
26. Hartl FU; Bracher A; Hayer-Hartl M Molecular chaperones in protein folding and proteostasis. *Nature* 2011, 475, 324–32. [PubMed: 21776078]
27. Horwich AL Molecular chaperones in cellular protein folding: the birth of a field. *Cell* 2014, 157, 285–8. [PubMed: 24725397]
28. Gestwicki JE; Shao H Inhibitors and chemical probes for molecular chaperone networks. *J. Biol. Chem* 2019, 294, 2151–2161. [PubMed: 30213856]
29. Kumar CMS; Mande SC; Mahajan G Multiple chaperonins in bacteria-novel functions and non-canonical behaviors. *Cell stress & chaperones* 2015, 20, 555–574. [PubMed: 25986150]
30. Lund PA Microbial molecular chaperones. *Adv Microb Physiol* 2001, 44, 93–140. [PubMed: 11407116]
31. Buchner J Molecular chaperones and protein quality control: an introduction to the JBC Reviews thematic series. *J. Biol. Chem* 2019, 294, 2074–2075. [PubMed: 30626733]
32. Fayet O; Ziegelhoffer T; Georgopoulos C The groES and groEL heat shock gene products of *Escherichia coli* are essential for bacterial growth at all temperatures. *J. Bacteriol* 1989, 171, 1379–85. [PubMed: 2563997]
33. Chapman E; Farr GW; Usaite R; Furtak K; Fenton WA; Chaudhuri TK; Hondorp ER; Matthews RG; Wolf SG; Yates JR; Pypaert M; Horwich AL Global aggregation of newly translated proteins in an *Escherichia coli* strain deficient of the chaperonin GroEL. *Proc. Natl. Acad. Sci. U.S.A* 2006, 103, 15800–5. [PubMed: 17043235]
34. Bittner AN; Foltz A; Oke V Only one of five groEL genes is required for viability and successful symbiosis in *Sinorhizobium meliloti*. *J. Bacteriol* 2007, 189, 1884–9. [PubMed: 17158666]
35. Kong TH; Coates ARM; Butcher PD; Hickman CJ; Shinnick TM Mycobacterium-Tuberculosis Expresses 2 Chaperonin-60 Homologs. *Proc. Natl. Acad. Sci. U.S.A* 1993, 90, 2608–2612. [PubMed: 7681982]

36. Hu YM; Henderson B; Lund PA; Tormay P; Ahmed MT; Gurcha SS; Besra GS; Coates ARM A Mycobacterium tuberculosis mutant lacking the groEL homologue cpn60.1 is viable but fails to induce an inflammatory response in animal models of infection. *Infect. Immun* 2008, 76, 1535–1546. [PubMed: 18227175]
37. Qamra R; Mande SC; Coates AR; Henderson B The unusual chaperonins of Mycobacterium tuberculosis. *Tuberculosis (Edinb)* 2005, 85, 385–94. [PubMed: 16253564]
38. Qamra R; Srinivas V; Mande SC Mycobacterium tuberculosis GroEL homologues unusually exist as lower oligomers and retain the ability to suppress aggregation of substrate proteins. *J. Mol. Biol* 2004, 342, 605–17. [PubMed: 15327959]
39. Hu YM; Coates ARM; Liu A; Lund PA; Henderson B Identification of the monocyte activating motif in Mycobacterium tuberculosis chaperonin 60.1. *Tuberculosis* 2013, 93, 442–447. [PubMed: 23643849]
40. Fan M; Rao T; Zacco E; Ahmed MT; Shukla A; Ojha A; Freeke J; Robinson CV; Benesch JL; Lund PA The unusual mycobacterial chaperonins: evidence for in vivo oligomerization and specialization of function. *Mol. Microbiol* 2012, 85, 934–44. [PubMed: 22834700]
41. Henderson B; Lund PA; Coates AR Multiple moonlighting functions of mycobacterial molecular chaperones. *Tuberculosis (Edinb)* 2010, 90, 119–24. [PubMed: 20338810]
42. Lund PA Multiple chaperonins in bacteria – why so many? *FEMS Microbiol. Rev* 2009, 33, 785–800. [PubMed: 19416363]
43. Horwich AL; Farr GW; Fenton WA GroEL-GroES-mediated protein folding. *Chem. Rev* 2006, 106, 1917–30. [PubMed: 16683761]
44. Horwich AL; Fenton WA Chaperonin-assisted protein folding: a chronologue. *Quarterly reviews of biophysics* 2020, 53, e4. [PubMed: 32070442]
45. Horwich AL; Fenton WA; Chapman E; Farr GW Two families of chaperonin: physiology and mechanism. *Annu. Rev. Cell. Dev. Biol* 2007, 23, 115–45. [PubMed: 17489689]
46. Horwich AL; Low KB; Fenton WA; Hirshfield IN; Furtak K Folding in-Vivo of Bacterial Cytoplasmic Proteins - Role of Groel. *Cell* 1993, 74, 909–917. [PubMed: 8104102]
47. Braig K; Otwinowski Z; Hegde R; Boisvert DC; Joachimiak A; Horwich AL; Sigler PB The crystal structure of the bacterial chaperonin GroEL at 2.8 Å. *Nature* 1994, 371, 578–86. [PubMed: 7935790]
48. Sigler PB; Xu Z; Rye HS; Burston SG; Fenton WA; Horwich AL Structure and function in GroEL-mediated protein folding. *Annu. Rev. Biochem* 1998, 67, 581–608. [PubMed: 9759498]
49. Fenton WA; Kashi Y; Furtak K; Horwich AL Residues in chaperonin GroEL required for polypeptide binding and release. *Nature* 1994, 371, 614–9. [PubMed: 7935796]
50. Fenton WA; Horwich AL GroEL-mediated protein folding. *Protein Sci.* 1997, 6, 743–60. [PubMed: 9098884]
51. Saibil HR; Fenton WA; Clare DK; Horwich AL Structure and allostery of the chaperonin GroEL. *J. Mol. Biol* 2013, 425, 1476–1487. [PubMed: 23183375]
52. Weissman JS; Hohl CM; Kovalenko O; Kashi Y; Chen S; Braig K; Saibil HR; Fenton WA; Horwich AL Mechanism of GroEL action: productive release of polypeptide from a sequestered position under GroES. *Cell* 1995, 83, 577–87. [PubMed: 7585961]
53. Weissman JS; Rye HS; Fenton WA; Beechem JM; Horwich AL Characterization of the active intermediate of a GroEL-GroES-mediated protein folding reaction. *Cell* 1996, 84, 481–90. [PubMed: 8608602]
54. Xu Z; Horwich AL; Sigler PB The crystal structure of the asymmetric GroEL-GroES-(ADP)7 chaperonin complex. *Nature* 1997, 388, 741–50. [PubMed: 9285585]
55. Johnson SM; Sharif O; Mak PA; Wang HT; Engels IH; Brinker A; Schultz PG; Horwich AL; Chapman E A biochemical screen for GroEL/GroES inhibitors. *Bioorg. Med. Chem. Lett* 2014, 24, 786–789. [PubMed: 24418775]
56. Abdeen S; Kunkle T; Salim N; Ray AM; Mammadova N; Summers C; Stevens M; Ambrose AJ; Park Y; Schultz PG; Horwich AL; Hoang QQ; Chapman E; Johnson SM Sulfonamido-2-arylbenzoxazole GroEL/ES Inhibitors as Potent Antibacterials against Methicillin-Resistant Staphylococcus aureus (MRSA). *J. Med. Chem* 2018, 61, 7345–7357. [PubMed: 30060666]

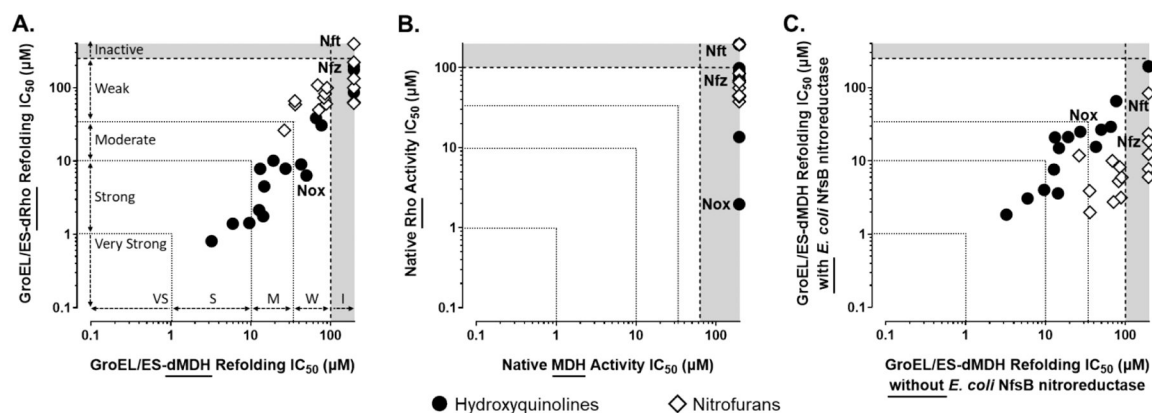
57. Abdeen S; Salim N; Mammadova N; Summers CM; Frankson R; Ambrose AJ; Anderson GG; Schultz PG; Horwich AL; Chapman E; Johnson SM GroEL/ES inhibitors as potential antibiotics. *Bioorg. Med. Chem. Lett* 2016, 26, 3127–34. [PubMed: 27184767]
58. Kunkle T; Abdeen S; Salim N; Ray AM; Stevens M; Ambrose AJ; Victorino J; Park Y; Hoang QQ; Chapman E; Johnson SM Hydroxybiphenylamide GroEL/ES Inhibitors Are Potent Antibacterials against Planktonic and Biofilm Forms of *Staphylococcus aureus*. *J. Med. Chem* 2018, 61, 10651–10664. [PubMed: 30392371]
59. Abdeen S; Salim N; Mammadova N; Summers CM; Goldsmith-Pestana K; McMahon-Pratt D; Schultz PG; Horwich AL; Chapman E; Johnson SM Targeting the HSP60/10 chaperonin systems of *Trypanosoma brucei* as a strategy for treating African sleeping sickness. *Bioorg. Med. Chem. Lett* 2016, 26, 5247–5253. [PubMed: 27720295]
60. Galloway SM; Raetz CR A mutant of *Escherichia coli* defective in the first step of endotoxin biosynthesis. *The Journal of biological chemistry* 1990, 265, 6394–402. [PubMed: 2180947]
61. Vuorio R; Vaara M The lipid A biosynthesis mutation lpxA2 of *Escherichia coli* results in drastic antibiotic supersusceptibility. *Antimicrob Agents Chemother* 1992, 36, 826–9. [PubMed: 1503445]
62. Abouelhassan Y; Yang Q; Yousaf H; Nguyen MT; Rolfe M; Schultz GS; Huigens RW 3rd. Nitroxoline: a broad-spectrum biofilm-eradicating agent against pathogenic bacteria. *Int J Antimicrob Agents* 2017, 49, 247–251. [PubMed: 28110918]
63. Thota S; Rodrigues DA; Pinheiro PSM; Lima LM; Fraga CAM; Barreiro EJ N-Acylhydrazones as drugs. *Bioorg. Med. Chem. Lett* 2018, 28, 2797–2806. [PubMed: 30006065]
64. Wagenlehner FM; Munch F; Pilatz A; Barmann B; Weidner W; Wagenlehner CM; Straubinger M; Blenk H; Pfister W; Kresken M; Naber KG Urinary concentrations and antibacterial activities of nitroxoline at 250 milligrams versus trimethoprim at 200 milligrams against uropathogens in healthy volunteers. *Antimicrob. Agents Chemother* 2014, 58, 713–21. [PubMed: 24217699]
65. Sobke A; Klinger M; Hermann B; Sachse S; Nietzsche S; Makarewicz O; Keller PM; Pfister W; Straube E The urinary antibiotic 5-nitro-8-hydroxyquinoline (Nitroxoline) reduces the formation and induces the dispersal of *Pseudomonas aeruginosa* biofilms by chelation of iron and zinc. *Antimicrob. Agents Chemother* 2012, 56, 6021–5. [PubMed: 22926564]
66. Kresken M; Korber-Irrgang B In vitro activity of nitroxoline against *Escherichia coli* urine isolates from outpatient departments in Germany. *Antimicrob. Agents Chemother* 2014, 58, 7019–20. [PubMed: 25182654]
67. Fuchs F; Wille J; Hamprecht A; Parcina M; Lehmann C; Schwarze-Zander C; Seifert H; Higgins PG In vitro activity of mecillinam and nitroxoline against *Neisseria gonorrhoeae* - re-purposing old antibiotics in the multi-drug resistance era. *J. Med. Microbiol* 2019, 68, 991–995. [PubMed: 31162022]
68. Muller AE; Verhaegh EM; Harbarth S; Mouton JW; Huttner A Nitrofurantoin's efficacy and safety as prophylaxis for urinary tract infections: a systematic review of the literature and meta-analysis of controlled trials. *Clin. Microbiol. Infect* 2017, 23, 355–362. [PubMed: 27542332]
69. Johnson SM; Petrassi HM; Palaninathan SK; Mohamedmohaideen NN; Purkey HE; Nichols C; Chiang KP; Walkup T; Sacchetti JC; Sharpless KB; Kelly JW Bisaryloxime ethers as potent inhibitors of transthyretin amyloid fibril formation. *Journal of medicinal chemistry* 2005, 48, 1576–87. [PubMed: 15743199]
70. Rando DG; Avery MA; Tekwani BL; Khan SI; Ferreira EI Antileishmanial activity screening of 5-nitro-2-heterocyclic benzylidene hydrazides. *Bioorg Med Chem* 2008, 16, 6724–31. [PubMed: 18571927]
71. Washburn A; Abdeen S; Ovechkina Y; Ray AM; Stevens M; Chitre S; Sivinski J; Park Y; Johnson J; Hoang QQ; Chapman E; Parish T; Johnson SM Dual-targeting GroEL/ES chaperonin and protein tyrosine phosphatase B (PtpB) inhibitors: A polypharmacology strategy for treating *Mycobacterium tuberculosis* infections. *Bioorganic & medicinal chemistry letters* 2019, 29, 1665–1672. [PubMed: 31047750]
72. Lopes AB; Miguez E; Kummerle AE; Rumjanek VM; Fraga CA; Barreiro EJ Characterization of amide bond conformers for a novel heterocyclic template of N-acylhydrazone derivatives. *Molecules* 2013, 18, 11683–704. [PubMed: 24071978]

73. Dinh NH; Tuyet Lan HT; Thu Trang TT; Van Hoan P Synthesis and NMR Spectroscopic Characteristics of a Series of Hydrazide-Hydrazones Containing Furoxan Ring Derived from Isoeugenoyacetic Acid. *Journal of Heterocyclic Chemistry* 2012, 49, 814–822.
74. Wiegand I; Hilpert K; Hancock RE Agar and broth dilution methods to determine the minimal inhibitory concentration (MIC) of antimicrobial substances. *Nat. Protoc* 2008, 3, 163–75. [PubMed: 18274517]
75. Miethke M; Marahiel MA Siderophore-based iron acquisition and pathogen control. *Microbiol Mol Biol Rev* 2007, 71, 413–51. [PubMed: 17804665]
76. du Moulinet d'Hardemare A; Gellon G; Philouze C; Serratrice G Oxinobactin and sulfoxinobactin, abiotic siderophore analogues to enterobactin involving 8-hydroxyquinoline subunits: thermodynamic and structural studies. *Inorg Chem* 2012, 51, 12142–51. [PubMed: 23134487]
77. Prachayasittikul V; Prachayasittikul S; Ruchirawat S; Prachayasittikul V 8-Hydroxyquinolines: a review of their metal chelating properties and medicinal applications. *Drug Des Devel Ther* 2013, 7, 1157–78.
78. Pelletier C; Prognon P; Bourlioux P Roles of divalent cations and pH in mechanism of action of nitroxoline against *Escherichia coli* strains. *Antimicrob. Agents Chemother* 1995, 39, 707–13. [PubMed: 7793877]
79. Nepali K; Lee HY; Liou JP Nitro-Group-Containing Drugs. *Journal of medicinal chemistry* 2019, 62, 2851–2893. [PubMed: 30295477]
80. Whiteway J; Koziarz P; Veall J; Sandhu N; Kumar P; Hoecher B; Lambert IB Oxygen-insensitive nitroreductases: analysis of the roles of *nfsA* and *nfsB* in development of resistance to 5-nitrofurantoin derivatives in *Escherichia coli*. *J. Bacteriol* 1998, 180, 5529–39. [PubMed: 9791100]
81. Kitamura S; Narai N; Tatsumi K Studies on bacterial nitroreductases. Enzymes involved in reduction of aromatic nitro compounds in *Escherichia coli*. *J. Pharmacobiodyn* 1983, 6, 18–24. [PubMed: 6343584]
82. Bryant DW; McCalla DR; Leeksa M; Laneuville P Type I nitroreductases of *Escherichia coli*. *Can. J. Microbiol* 1981, 27, 81–6. [PubMed: 7011517]
83. Roldan MD; Perez-Reinado E; Castillo F; Moreno-Vivian C Reduction of polynitroaromatic compounds: the bacterial nitroreductases. *FEMS Microbiol. Rev* 2008, 32, 474–500. [PubMed: 18355273]
84. Stevens M; Abdeen S; Salim N; Ray AM; Washburn A; Chitre S; Sivinski J; Park Y; Hoang QQ; Chapman E; Johnson SM HSP60/10 chaperonin systems are inhibited by a variety of approved drugs, natural products, and known bioactive molecules. *Bioorganic & medicinal chemistry letters* 2019, 29, 1106–1112. [PubMed: 30852084]
85. Race PR; Lovering AL; Green RM; Ossor A; White SA; Searle PF; Wrighton CJ; Hyde EI Structural and mechanistic studies of *Escherichia coli* nitroreductase with the antibiotic nitrofurazone. Reversed binding orientations in different redox states of the enzyme. *J. Biol. Chem* 2005, 280, 13256–64. [PubMed: 15684426]
86. Chapman E; Farr GW; Fenton WA; Johnson SM; Horwich AL Requirement for binding multiple ATPs to convert a GroEL ring to the folding-active state. *Proceedings of the National Academy of Sciences of the United States of America* 2008, 105, 19205–10. [PubMed: 19050077]
87. Chapman E; Farr GW; Furtak K; Horwich AL A small molecule inhibitor selective for a variant ATP-binding site of the chaperonin GroEL. *Bioorganic & medicinal chemistry letters* 2009, 19, 811–3. [PubMed: 19110421]
88. Kim S; Lieberman TD; Kishony R Alternating antibiotic treatments constrain evolutionary paths to multidrug resistance. *Proc. Natl. Acad. Sci. U.S.A* 2014, 111, 14494–9. [PubMed: 25246554]



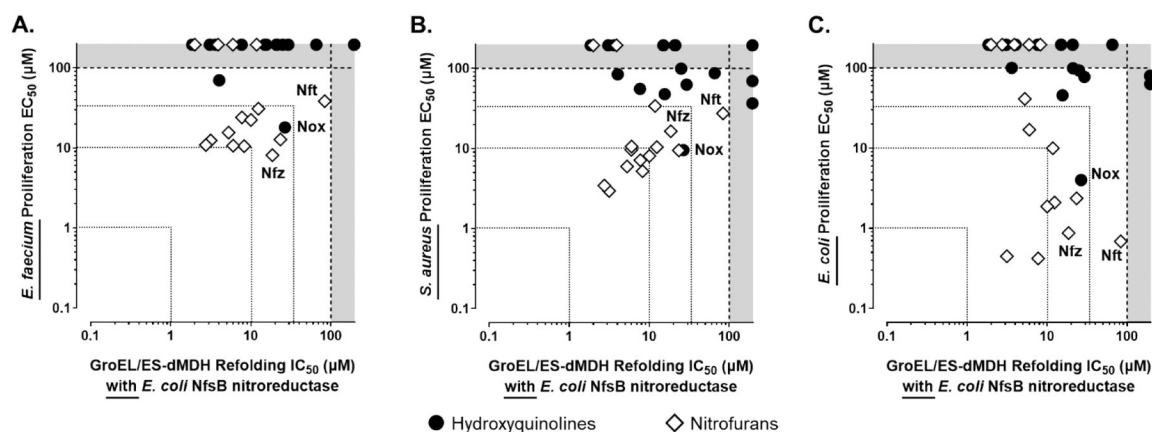
**Figure 1.**

Previous investigations identified *bis*-sulfonamido-2-phenylbenzoxazole (**BSP**) and salicylanilide (**SCA**) analogs that were potent GroEL/ES inhibitors with antibacterial activity against Gram-positive bacteria.<sup>56–59</sup> Compound **1** was previously found to be a moderate inhibitor of GroEL/ES-mediated refolding of denatured rhodanese and malate dehydrogenase substrates ( $IC_{50} = 18$  &  $31$   $\mu$ M, respectively) and a weak to moderate inhibitor of the proliferation of *B. subtilis* ( $EC_{50} = 83$   $\mu$ M), methicillin-resistant *S. aureus* ( $EC_{50} = 56$   $\mu$ M), *K. pneumoniae* ( $EC_{50} = 95$   $\mu$ M), *A. baumannii* ( $EC_{50} = 32$   $\mu$ M), and SM101 *E. coli* ( $EC_{50} = 19$   $\mu$ M).<sup>55, 57</sup> Owing to its ability to inhibit both Gram-positive and Gram-negative bacteria, and its structural similarity to known antibacterials nitroxoline, nifuroxazide, and nitrofurantoin, in this study, we sought to develop new compound **1** analogs (Scheme 1) that were more potent and selective inhibitors of GroEL/ES and bacterial proliferation.



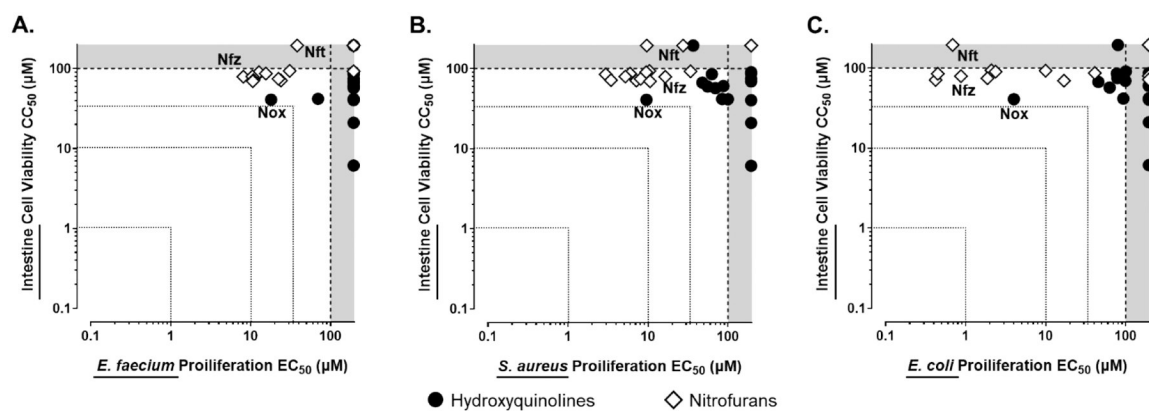
**Figure 2.**

Correlation plots of IC<sub>50</sub> values for compounds evaluated in the respective biochemical assays. **A.** Compounds inhibited nearly equipotently in the GroEL/ES-dMDH and the GroEL/ES-dRho refolding assays (Spearman correlation coefficient comparing log(IC<sub>50</sub>) values in each assay is 0.8877 ( $p < 0.0001$ )). For the purposes of categorizing inhibitor potencies, we consider compounds with IC<sub>50</sub> values plotted in the grey zones to be inactive (i.e. greater than the maximum concentrations tested), >33 μM to be weak inhibitors, 11–33 μM moderate inhibitors, 1–11 μM potent inhibitors, and <1 μM very potent and acting near stoichiometrically since the concentration of GroEL tetradecamer is 50 nM during the refolding cycle (i.e. 700 nM GroEL monomeric subunits). **B.** While some compounds inhibited in the native Rho enzymatic reporter counter-screen, none inhibited native MDH enzymatic activity, supporting that inhibitors were not false-positives that simply target the enzymatic reporter reactions of the coupled GroEL/ES-mediated refolding assays. **C.** Nitrofuran analogs exhibited increased inhibition in the GroEL/ES-dMDH refolding assay in the presence of *E. coli* NfsB, while hydroxyquinoline analogs did not (Spearman correlation coefficient comparing hydroxyquinoline log(IC<sub>50</sub>) values in each assay is 0.9527 ( $p < 0.0001$ )), supporting a pro-drug mechanism of action through metabolism of the nitro group. No compounds inhibited native MDH enzymatic activity in either the absence or presence of *E. coli* NfsB (refer to Table S1 in the Supporting Information). Results plotted in the grey zones represent IC<sub>50</sub> values higher than the maximum concentrations tested. Data points for nifuroxazide (**Nfz**), nitrofurantoin (**Nft**), and nitroxoline (**Nox**) are labelled for comparison.



**Figure 3.**

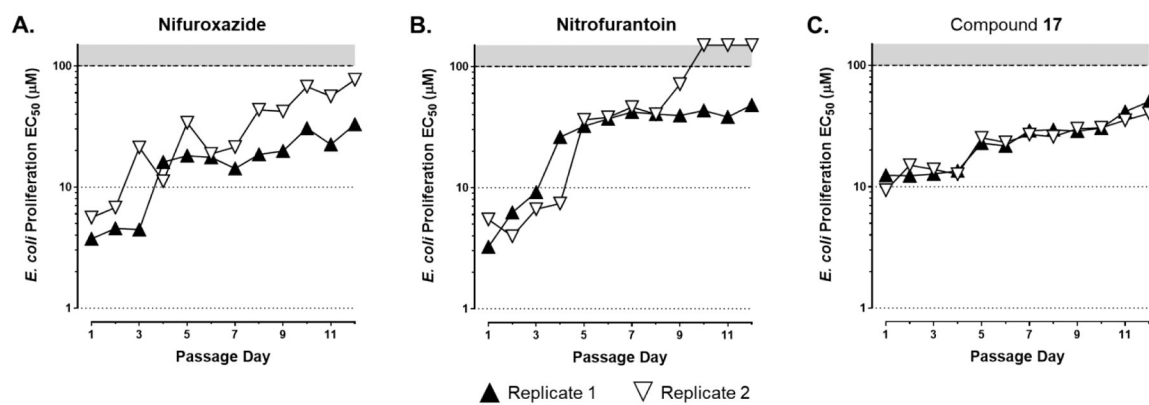
Correlation plots comparing IC<sub>50</sub> values for compounds tested in the *in situ* NfsB-GroEL/ES-dMDH refolding assay with EC<sub>50</sub> values for inhibiting *E. faecium* (A), *S. aureus* (B), and *E. coli* (C) proliferation. While increasing inhibition by the nitrofurans in the *in situ* NfsB-GroEL/ES-dMDH refolding assay in general provided more effective inhibition of *S. aureus* growth (panel B), more thorough studies will need to be conducted – e.g. testing a larger number of analogs in the presence of *S. aureus* nitroreductases and GroEL/ES chaperonin system – to gain a clearer picture of whether or not compounds may be functioning on-target against GroEL/ES in bacteria. Results plotted in the grey zones represent IC<sub>50</sub> and EC<sub>50</sub> values higher than the maximum concentrations tested. Data points for nifuroxazide (Nfz), nitrofurantoin (Nft), and nitroxoline (Nox) are labelled for comparison.



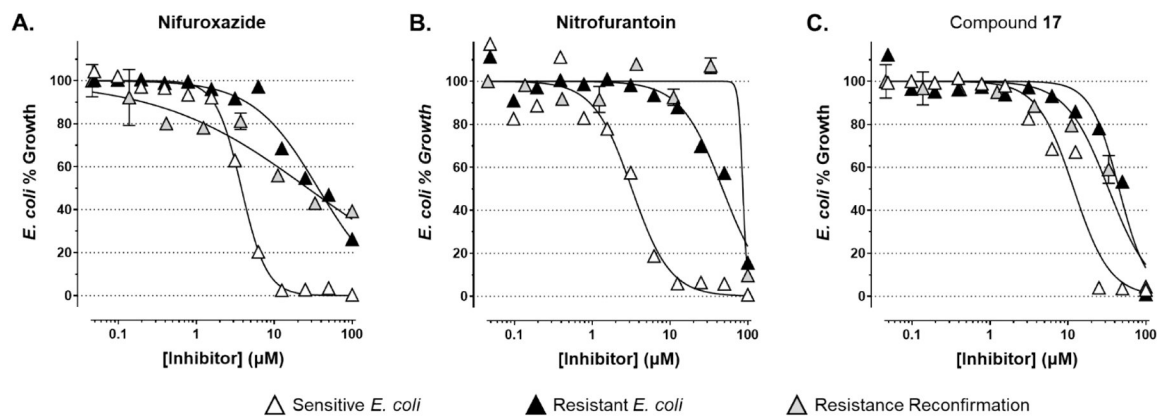
**Figure 4.**

Correlation plots examining the selectivity of compounds inhibiting the proliferation of *E. faecium* (A), *S. aureus* (B), and *E. coli* (C) over cytotoxicity to human FHs 74 Int small intestine cells (results for cytotoxicity to human FHC colon cells are similar, with  $CC_{50}$  values reported in Table S2 and Figure S1 in the Supporting Information). Results plotted in the grey zones represent  $EC_{50}$ , and  $CC_{50}$  values higher than the maximum concentrations listed. Data points for nifuroxazide (Nfz), nitrofurantoin (Nft), and nitroxoline (Nox) are labelled for comparison.

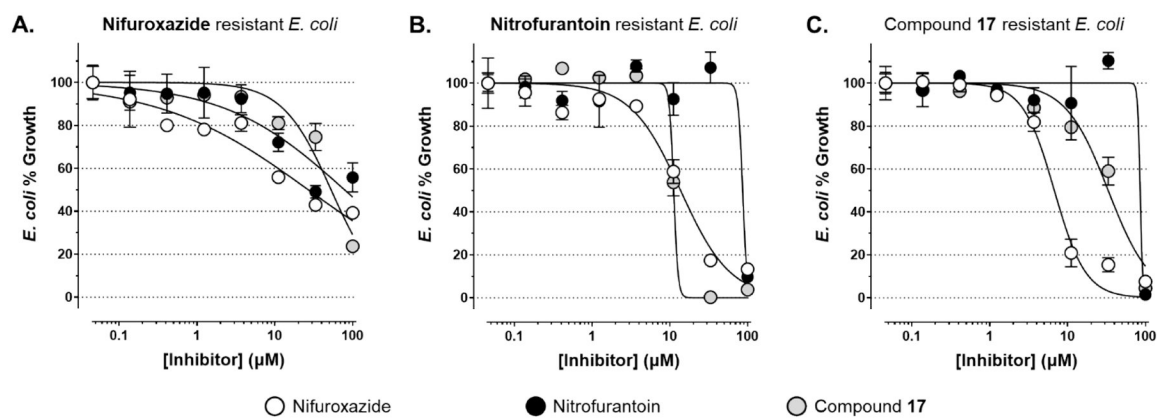




**Figure 5.** Evaluating the ability of *E. coli* to generate resistance to nifuroxazide (A), nitrofurantoin (B), and compound 17 (C) over time. Time-course plots show the change in EC<sub>50</sub> values for each compound over the 12-day serial passage resistance assay (compounds tested in duplicates, as indicated by the black and white triangles).

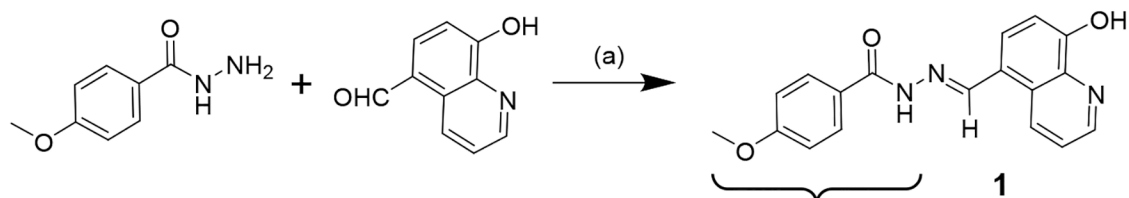
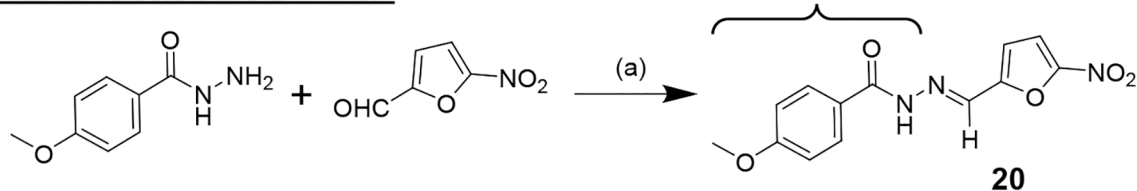
**Figure 6.**

Dose-response curves for nifuroxazide (A), nitrofurantoin (B), and compound 17 (C) tested against the susceptible parent *E. coli* (white triangle), the maximally-resistant strains developed to the respective test compounds (black triangle), and follow-up proliferation assays for resistant strains tested after serial passaging in the absence of test compounds to account for possible reversible inhibition mechanisms (grey triangles). Results are presented for the replicate 1 samples from the resistance assay, with results for replicate 2 samples similar and presented in Figure S2 in the Supporting Information. In all instances, the resistant strains were nearly equally resistant even after culturing in the absence of inhibitors for the 4×12 h passages.



**Figure 7.**

Evaluation of cross-resistance between the respective resistant *E. coli* strains with nifuroxazide, nitrofurantoin, and compound **17**. The three panels show dose-response curves for the three inhibitors tested against strains where resistance was initially generated to nifuroxazide (A), nitrofurantoin (B), and compound **17** (C). Results are presented for the replicate 1 samples from the resistance assay, with results for replicate 2 samples similar and presented in Figure S3 in the Supporting Information. Results indicate that resistance generated to one inhibitor is not necessarily cross-resistant to the other inhibitors, potentially indicating different mechanisms of activation and/or targets.

Hydroxyquinoline (HQ) Series: 1-15Nitrofurans (NF) Series: 16-28**Scheme 1a.**

Structures of the hydroxyquinoline (HQ – 1–15) and nitrofurans (NF – 16–28, including nitrofurantoin and nifuroxazide) series of analogs with the syntheses of compounds **1** and **20** shown as a representative examples. To develop SAR in each series, the methoxy rings of **1** and **20** were substituted with a variety of other ring substructures that we have found effective with other GroEL/ES inhibitor scaffolds that have shown antibacterial properties (e.g. thiophenes, 2-chlorothiophenes, and aryl-sulfonamides) – please refer to the data tables in the Supporting Information for specific compound structures.<sup>69, 70</sup>

<sup>a</sup> Reagents and conditions: (a) The respective hydrazides and aldehydes were stirred with cat. HCl in DMSO for 18 h, then precipitated in water, filtered, and dried *in vacuo* (46–99% yields).

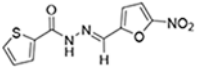
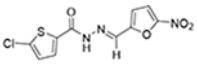
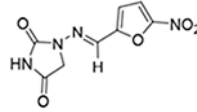
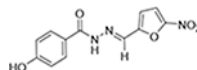
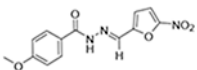
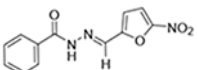
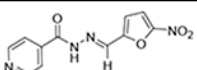
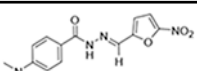
**Table 1.**

Compilation of EC<sub>50</sub> values for the hydroxyquinoline and nitrofurans tested in the *ESKAPE* and *E. coli* bacterial proliferation assays. Cells that are shaded darker blue are most potent, while those that are shaded lighter blue to white are less potent to inactive (>100 μM).

	#	<i>E. faecium</i>	<i>S. aureus</i>	<i>K. pneumoniae</i>	<i>A. baumannii</i>	<i>P. aeruginosa</i>	<i>E. cloacae</i>	<i>E. coli</i>	
<b>Hydroxyquinolines</b>	2	>100	37	>100	>100	>100	>100	80	
	3	>100	63	99	74	>100	92	77	
	4	70	84	>100	>100	>100	>100	>100	
	5	>100	69	82	56	>100	80	63	
	6	>100	>100	>100	>100	>100	>100	79	
	7	>100	48	87	71	>100	97	46	
	1	>100	87	85	>100	95	100	>100	
	8	>100	99	>100	>100	>100	>100	93	
	9	>100	56	>100	>100	>100	>100	>100	
	10	>100	>100	>100	>100	81	>100	>100	
	11	>100	>100	>100	>100	>100	>100	>100	
	12	>100	>100	>100	>100	85	>100	99	
	13	>100	>100	>100	>100	>100	>100	>100	
	14	>100	>100	>100	84	>100	>100	100	
	15	>100	>100	>100	>100	>100	>100	>100	
	Nitroxoline	18	9.5	2.8	2.5	99	6.6	4.0	
<b>Nitrofurans</b>		Nitrofurantoin	38	27	40	>100	>100	36	0.69
	16	24	7.1	16	82	>100	40	0.42	
	17	12	3.0	19	72	>100	49	0.45	
	18	31	10	36	>100	>100	>100	2.1	
	19	13	9.5	42	54	>100	73	2.4	
		Nifuroxazide	8.1	16	37	>100	>100	54	0.87
	20	22	8.1	>100	>100	>100	>100	1.9	
	21	>100	34	>100	>100	>100	>100	10.0	
	22	16	6.0	>100	>100	>100	>100	41	
	23	11	5.2	>100	>100	>100	>100	>100	
	24	11	3.5	>100	>100	>100	>100	>100	
	25	>100	9.6	>100	>100	>100	>100	>100	
	26	11	11	>100	>100	>100	>100	17	
27	>100	>100	>100	>100	>100	>100	>100		
28	>100	>100	>100	>100	>100	>100	>100		

**Table 2.**

Cell-based and biochemical EC<sub>50</sub>, CC<sub>50</sub>, and IC<sub>50</sub> results for the top eight lead inhibitors based on average Selectivity Indices (SI) for inhibiting *E. coli* proliferation over cytotoxicity to human colon and intestine cells. For the GroEL/ES-dMDH refolding assay and native MDH counter-screens, IC<sub>50</sub> results are shown for compounds tested in the absence and presence of NfsB nitroreductase (w/ and w/o NR, respectively).

Compound Structure & Name / Number	Cell-Based Assay EC <sub>50</sub> & CC <sub>50</sub> (μM)											Biochemical Assay IC <sub>50</sub> (μM)				
	Bacterial Proliferation							Human Cell Viability		SI (CC <sub>50</sub> / EC <sub>50</sub> )		Native MDH		GroEL/ES-dMDH refolding:		
	<i>E</i>	<i>S</i>	<i>K</i>	<i>A</i>	<i>P</i>	<i>E</i>	<i>E. coli</i>	Colon	Intestine	Colon	Intestine	w/o NR	w/ NR	w/o NR	w/ NR	
	16	24	7.1	16	82	>100	40	0.42	83	71	198	168	>63	>56	>100	7.7
	17	12	3.0	19	72	>100	49	0.45	53	85	119	190	>63	>56	88	3.2
		38	27	40	>100	>100	36	0.69	>100	>100	>146	>146	>63	>56	>100	84
Nitrofurantoin																
		8.1	16	37	>100	>100	54	0.87	61	79	70	91	>63	>56	>100	19
Nifuroxazide																
	20	22	8.1	>100	>100	>100	>100	1.9	>100	75	>53	40	>63	>56	69	10
	18	31	10	36	>100	>100	>100	2.1	>100	94	>48	45	>63	>56	>100	12
	19	13	9.5	42	54	>100	73	2.4	61	90	26	38	>63	>56	>100	23
	21	>100	34	>100	>100	>100	>100	10.0	>100	93	>10	9.3	>63	>56	26	12